First-principles study of diffusion of Li, Na, K and Ag in ZnO

2009 J. Phys.: Condens. Matter 21 345802

(http://iopscience.iop.org/0953-8984/21/34/345802)

J. Phys.: Condens. Matter **21** (2009) 345802 (7pp) doi:10.1088/0953-8984/21/34/345802

First-principles study of diffusion of Li, Na, K and Ag in ZnO

Gui-Yang Huang[1], **Chong-Yu Wang**[1,2] **and Jian-Tao Wang**[3]

[1] Department of Physics, Tsinghua University, Beijing 100084, People's Republic of China
[2] The International Centre for Materials Physics, Chinese Academy of Sciences, Shenyang 110016, People's Republic of China
[3] Institute of Physics, Chinese Academy of Sciences, Beijing 100080, People's Republic of China

Received 5 March 2009, in final form 24 June 2009
Published 5 August 2009
Online at stacks.iop.org/JPhysCM/21/345802

Abstract

Based on *ab initio* total energy calculations, Li, Na and Ag interstitials are found to be stable with at least a 1.56 eV energy barrier to transform to a zinc substitutional site in ZnO, whereas K interstitial has a relatively small energy barrier at 0.79 eV. The isolated dopant substitutional defects (Li_{Zn}, Na_{Zn}, K_{Zn} and Ag_{Zn}) are found to be rather stable, with at least a 3.4 eV energy barrier to transform to an interstitial site. All of the dopant interstitials (Li_i, Na_i, K_i and Ag_i) are fast diffusers. The diffusion of Li interstitial is isotropic, whereas the diffusion of Na, K and Ag interstitials is highly anisotropic. Fundamental processes of the vacancy-assisted mechanisms are systematically investigated and specific values of the energy barriers are obtained.

(Some figures in this article are in colour only in the electronic version)

1. Introduction

Zinc oxide (ZnO), with a wide bandgap (3.44 eV) and large exciton binding energy (60 meV), has been of great interest for potential applications in optical and optoelectronic devices [1]. The stable and reproducible p-type doping is the key problem for these applications. Group I elements (Li, Na, K, Ag) substituting for Zn are one main class of candidate for p-type doping [2–4]. When these dopant atoms are introduced into the ZnO films, their subsequent redistribution by diffusion is almost inevitable in the processing steps that follow. The doping behaviors of Li have been investigated comprehensively by Wardle *et al* [5], whereas there are still some remaining issues which have not been touched on, for example, the stability of Li interstitial (Li_i) and Li substitutional (Li_{Zn}), as well as the vacancy-assisted diffusion mechanism. For Na, K and Ag, the diffusion and stability studies are much more limited. The diffusion and stability properties of these dopants are essential for understanding their p-type doping behavior and a systematic theoretical investigation is highly desirable.

The purpose of the present work is to investigate the diffusion behavior of Li, Na, K and Ag in ZnO. First, we investigate the stability of Li, Na, K and Ag interstitials and substitutionals, by calculating the annihilation barrier under isolated conditions (no other defects present nearby), where the annihilation barrier is defined as the energy barrier of transformation to other types of configuration. Second, we investigate the diffusion behavior of Li, Na, K and Ag interstitials. Third, we investigate the vacancy-assisted mechanisms of Li, Na, K and Ag diffusion, which is one of the most common means of atomic diffusion in crystalline solids for substitutional dopants.

2. Calculational method and models

The density functional calculations were carried out using the plane-wave-based Vienna *ab initio* simulation package (VASP) [6, 7], based on the generalized-gradient approximation (GGA) with the functional of Perdew, Burke and Ernzerhof (PBE) [8]. The electron wavefunctions were described using the projector augmented wave (PAW) method of Blöchl [9] in the implementation of Kresse and Joubert [10]. Plane waves have been included up to a cutoff energy of 400 eV. Electronic states were occupied with a Gaussian smearing width of 0.05 eV. A real-space projection scheme was used for efficient computation. Orthogonal supercells containing 96 atoms were employed, with $a1 = 11.40$ Å, $a2 = 9.87$ Å and $a3 = 10.62$ Å, which had lattice vectors $(0, 2\sqrt{3}a, 0)$, $(3a, 0, 0)$ and $(0, 0, 2c)$. All calculations were carried out at the theoretical constant of bulk wurtzite ZnO. For integration within the Brillouin zone specific k-points were selected

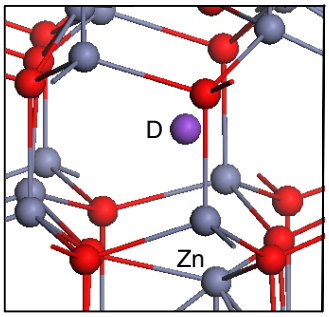

Figure 1. Schematic local atomic geometry of K and Ag split interstitials. D denotes K or Ag. D is located at the hexagonal channel of the wurzite structure, but not at the center of the hexagonal channel. It approaches and noticeably pushes downwards one of the nearest-neighbors Zn atoms along the *c* axis.

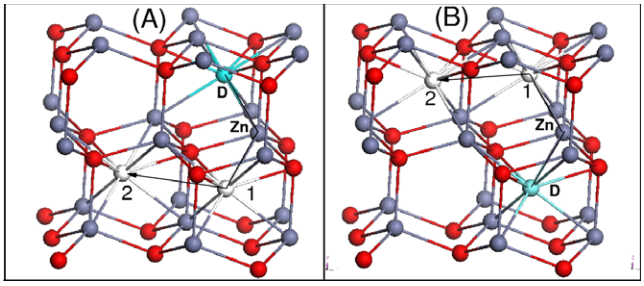

Figure 2. Schematic kick-out processes. (A) Kick-out downwards along the *c* axis. (B) Kick-out upwards along the *c* axis. The dopant atom first kicks out Zn to site 1, and then diffuses to site 2. D denotes dopant atom. Site D, site 1 and site 2 are the octahedral interstitial sites of the wurzite structure.

using 2 × 2 × 2 Monkhorst–Pack grids. The optimization procedure was truncated when the residual forces for the relaxed atoms were less than 0.01 eV Å^{-1}. The zinc 3d electrons were explicitly included in our calculations. For charged defects, a jellium background charge is added automatically by VASP to neutralize the supercell. In addition, to calculate the binding energy of a dopant–vacancy pair, orthogonal supercells containing 192 atoms were employed, with $a1 = 11.40$ Å, $a2 = 19.74$ Å and $a3 = 10.62$ Å. For integration within the Brillouin zone specific *k*-points were selected using 2 × 1 × 2 Monkhorst–Pack grids.

In order to obtain the energy barriers for the various diffusion paths we employed the climbing image nudged elastic band method [11, 12], as implemented in VASP by Henkelman, Jonsson and others[4]. The images of the CI-NEB were relaxed until the maximum residual force was less than 0.01 eV Å^{-1}.

In addition, the binding energy of a dopant–vacancy pair is obtained by taking the energy difference between the total energy of the 192-atom supercell with a dopant–vacancy pair and the dopant with the furthest zinc vacancy in the 192-atom supercell.

3. Results and discussion

3.1. Stability of Li, Na, K and Ag interstitials

First, we check the atomic geometry of Li, Na, K and Ag interstitials of +1 charge state. Both Li_i and Na_i tend to occupy the symmetric octahedral interstitial site (similar to Zn_i [16], at the center of the hexagonal channel), whereas K_i and Ag_i tend to occupy the so-called interstitialcy site (also called the dumbbell interstitial, split interstitial or nonsymmetric interstitial), as shown in figure 1, which an interstitialcy defect consisting of two atoms (in nonsubstitutional positions) on a single substitutional lattice site [15]. For Na_i, there is also such a nonsymmetric octahedral interstitial site: however, it has about 0.1 eV higher energy. We also check Li_i carefully and find no nonsymmetric configuration for it. Except for Li_i (with very small atomic radius), we noticed that other dopant interstitials commonly have two nonequivalent configurations at the octahedral interstitial site. For more or less smaller atoms Zn_i^{2+} [16], Li_i^{1+} and Na_i^{1+}, the symmetric octahedral interstitial has smaller energy than the nonsymmetric one. For larger atoms like Ga_i^{3+} [18], K_i^{1+} and Ag_i^{1+}, the symmetric octahedral interstitial is not stable, and is readily relaxed to the nonsymmetric octahedral interstitial configuration. For Ag_i, the nonsymmetric configuration has about 0.57 eV lower energy. For K_i, the symmetric configuration is highly unstable.

In order to investigate the stability of the Li, Na, K and Ag interstitials, we calculate the energy barrier of the kick-out processes where the dopant kicks the nearest-neighbor Zn out to an octahedral interstitial site. Due to the wurzite structure of ZnO, there are two main types of kick-out processes, upwards and downwards along the *c* axis, as shown in figure 2.

For Li and Na, Zn_i in the first-nearest-neighbor octahedral interstitial of Li_{Zn} is unstable. It is necessary to consider the processes when the generated Zn_i diffuses away from Li_{Zn} to another octahedral interstitial site, as shown in figure 2. Calculated energies along the migration paths are shown in figure 3. We can see that both Li_i and Na_i have a large annihilation barrier (kick-out barrier). For kick-out path B, shown in figures 2(B) and 3(B), the final state is still very unstable (with a small escape barrier). Therefore, we should use the energy barrier of kick-out path A, shown in figures 2(A) and 3(A), to determine the annihilation barrier, which is 2.19 eV for Li_i and 1.60 eV for Na_i.

For K, it occupies the so-called interstitialcy site, as shown in figure 1. For simplicity, the schematic kick-out processes are also shown in figure 2. In addition, we also investigate the process whereby the kick-out-generated Zn_i diffuses away by the kick-out mechanism, as shown in figure 4. Calculated energies along the migration paths are shown in figure 5. We can see that, though K can kick out Zn to the first-nearest-neighbor site (site 1 shown in figure 2(A)) with a very small energy barrier of 0.19 eV for kick-out path (A) (shown in figures 2(A) and 5(A)), the generated Zn interstitial has to overcome an 0.69 eV extra energy barrier to diffuse away (site 1 to site 2, shown in figure 2(A)). For the Zn_i kick-out pathway (site 1 to site 3, shown in figure 4), the energy barrier is also more or less the same, 0.6 eV. In dopant-free wurzite ZnO, these two diffusion pathways have very small energy

[4] The implementations of the climbing image nudged elastic band and the dimer method for VASP were obtained from [13].

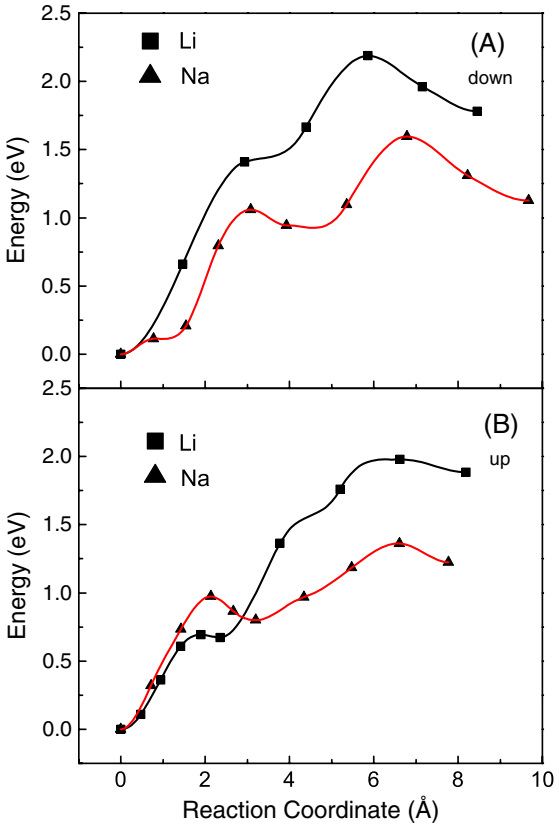

Figure 3. Calculated energy along the kick-out processes for Li and Na. (A) Kick-out downwards along the *c* axis. (B) Kick-out upwards along the *c* axis.

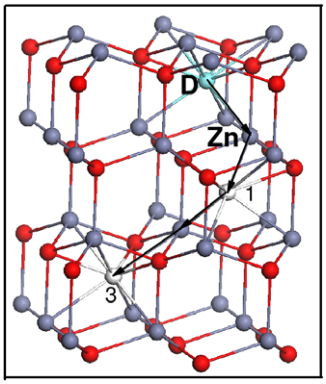

Figure 4. Schematic kick-out process. The dopant atom first kicks out Zn downwards to site 1. Then the generated Zn interstitial in site 1 kicks out the neighbor Zn downwards to site 3. D denotes dopant atom. Site D, site 1, site 2 and site 3 are the octahedral interstitial sites of the wurzite structure.

barriers, which are 0.34 eV and 0.36 eV, respectively [16]. In the present work, we also recalculated the former process and obtained almost the same value, 0.33 eV. (It indicates that GGA (PW91) and GGA (PBE) generate almost the same results.) Combining all these factors, the annihilation barrier of K_i is 0.79 eV (corresponding to process A in figure 5).

For Ag, it occupies the so-called interstitialcy site, as shown in figure 1, similar to K. The kick-out processes for

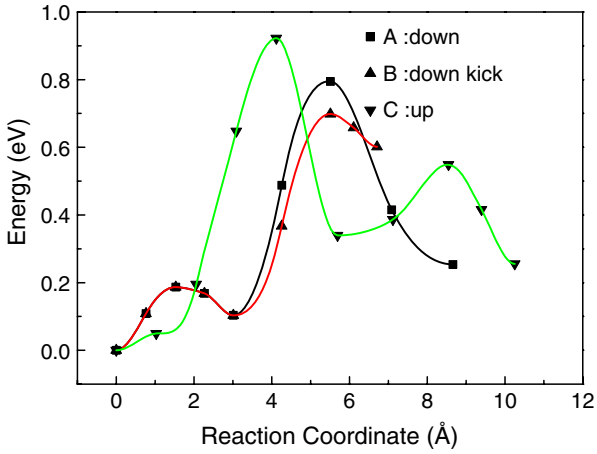

Figure 5. Calculated energy along the kick-out processes for K. (A) Kick-out downwards along the *c* axis, corresponding to process (A) in figure 2. (B) Kick-out downwards along the *c* axis, corresponding to the process in figure 4. (C) Kick-out upwards along the *c* axis, corresponding to process (B) in figure 2.

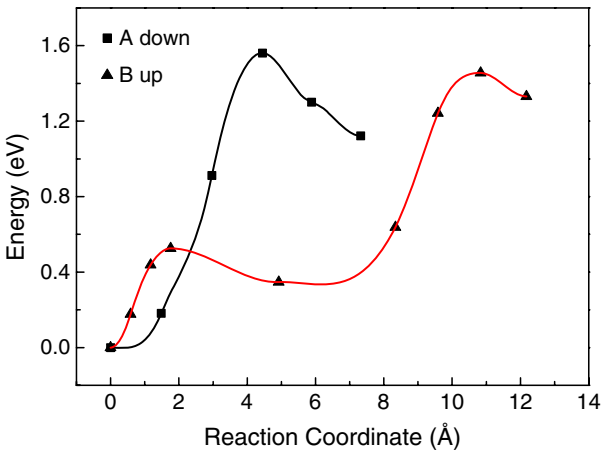

Figure 6. Calculated energy along the kick-out processes for Ag. (A) Kick-out downwards along the *c* axis, corresponding to process (A) in figure 2. (B) Kick-out upwards along the *c* axis, corresponding to process (B) in figure 2.

Ag are rather complicated and have many different pathways. For simplicity, two kick-out processes are schematically shown in figure 2 as well. Different from K, there is no clear configuration of Zn_i in site 1 shown in figure 2. So the actual kick-out processes are very different from the processes shown in figure 2. The detailed description of these processes is not shown here, as it is more or less irrelevant for our conclusions. Calculated energies along the migration paths are shown in figure 6. We noticed that the final state of the kick-out processes has at least 1.12 eV higher energy, which indicates that the kick-out barrier cannot be smaller than 1.12 eV. In summary, the annihilation barrier of Ag_i is 1.56 eV (corresponding to process A in figure 6).

In summary, all of these dopant interstitials are not easy to occupy the substitutional site by kicking out neighboring zinc to an octahedral interstitial site. The smaller the atomic radius, the larger the kick-out barrier. Furthermore, the

attractive interaction between the dopant substitutional and zinc interstitial seems to contribute a lot to the kick-out barrier. For Li, Na and Ag, since the kick-out energies are at least as large as 1.56 eV, if they are introduced initially in the interstitial site via diffusion doping or ion implantation, the Li_{Zn}, Na_{Zn} and Ag_{Zn} may not reach or maintain equilibrium concentration.

In addition, we also investigate the binding energy of the dopant (Li, Na, K, Ag and Rb) and zinc interstitial pairs by calculating the energy difference between 192-atom supercells with a dopant–interstitial pair and a dopant with the furthest zinc interstitial in the 192-atom supercell (LDA). The calculated binding energy (Li, Na, K, Ag and Rb) is 1.09 eV, 1.07 eV, 1.34 eV, 2.04 eV and 1.22 eV, respectively. For Rb, it is very easy to kick the nearest-neighbor Zn out to the octahedral interstitial site with a smaller than 0.1 eV energy barrier, and the final configuration has about 0.53 eV lower energy. Ag is special and there is no clear configuration of Zn_i in site 1 shown in figure 2. For Li, Na, K and Rb, the dopant–interstitial pair is actually the configuration shown in figure 2(A), where the dopant (Li, Na, K and Rb) occupies the substitutional site and Zn_i in site 1. Combining the kick-out energy and binding energy, we can obtain the energy that the dopant interstitial transforms to the zinc substitutional site and generates one zinc interstitial (far away from the dopant), which is about 2.59 eV, 2.04 eV, 1.97 eV, 1.44 eV and 0.69 eV for Li, Ag, Na, K and Rb, respectively. Although Rb has a large atomic radius, we find it has a shallow acceptor level. To date, Rb has never been used for p-type doping in ZnO.

3.2. Diffusion behavior of Li, Na, K and Ag interstitials

Second, we investigate the diffusion behavior of Li, Na, K and Ag interstitials of +1 charge state, including both parallel and perpendicular to the *c* axis. For Li_i, it migrates perpendicular to the *c* axis across the metastable tetrahedral interstitial site with a 0.68 eV energy barrier (different from the diffusion of the zinc interstitial [16], because there is no nonsymmetric metastable configuration for Li, as discussed above), as well as parallel to the *c* axis with a 0.61 eV energy barrier, as shown in figure 7, in good agreement with the 0.64 and 0.58 eV obtained by Wardle *et al* [5]. For Na_i, the tetrahedral interstitial site is not stable. We found Na_i does not migrate through the tetrahedral interstitial site, but migrates perpendicular to the *c* axis with a 0.74 eV energy barrier, more or less straight to the neighboring octahedral interstitial by noticeably pushing down the nearest-neighbor Zn, which is similar to the diffusion of zinc interstitial [16] (because both of them have one metastable nonsymmetric configuration as discussed above and in [16]), as well as parallel to the *c* axis with a 1.33 eV energy barrier, as shown in figure 7. For K_i, it migrates perpendicular to the *c* axis in the same octahedral interstitial cage with a 0.18 eV energy barrier and migrates perpendicular to the *c* axis to the nearest-neighbor octahedral interstitial cage with a less than 0.1 eV energy barrier, as well as migrates parallel to the *c* axis with a 1.49 eV energy barrier, as shown in figure 8. It indicates that K can diffuse very easily perpendicular to the *c* axis, with a 0.18 eV overall energy barrier. For Ag_i, it migrates perpendicular to the *c* axis in the same octahedral interstitial cage with a 0.35 eV energy barrier and migrates perpendicular to the *c* axis to the nearest-neighbor octahedral interstitial cage with a less than 0.1 eV energy barrier, as well as migrates parallel to the *c* axis with a 0.98 eV energy barrier, as shown in figure 8. We can see a large anisotropic diffusion behavior for Na_i, K_i and Ag_i. All of the dopant interstitials (Li_i, Na_i, K_i and Ag_i) are fast diffusers. It indicates that the concentration of these dopant interstitials is proposed to be in an equilibrium state.

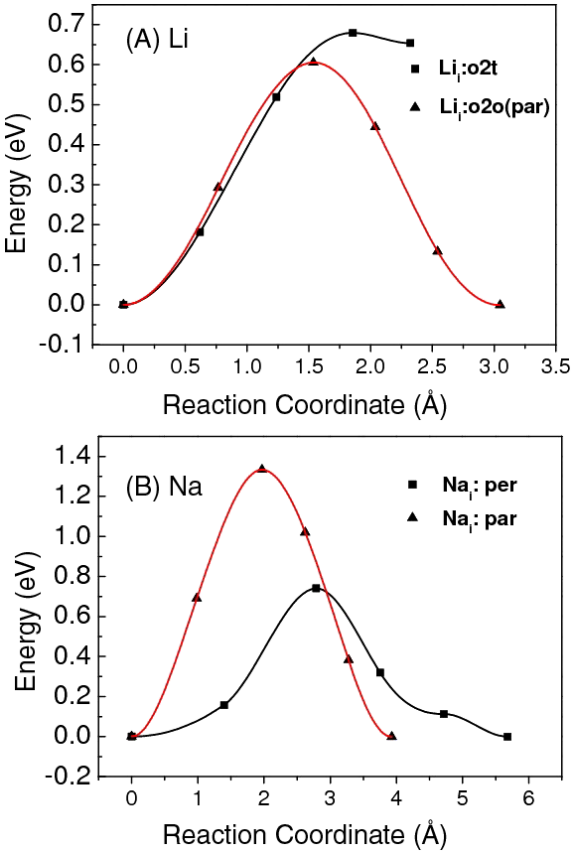

Figure 7. Calculated energy along the migration paths for Li and Na, perpendicular to the *c* axis and parallel to the *c* axis. Li_i:o2t denotes Li migrates from the octahedral site to the tetrahedral site perpendicular to the *c* axis.

3.3. Stability of Li_{Zn}, Na_{Zn}, K_{Zn} and Ag_{Zn} interstitial

In order to investigate the stability of Li_{Zn} (Li substituting for Zn), we calculate the energy barrier of the dissociation processes of Li_{Zn} to Li_i (generating a V_{Zn}) for both the −1 charge state and neutral charge state, which is 3.41 eV and 3.24 eV, respectively, as shown in figure 9. It indicates that the isolated Li_{Zn} is rather stable. According to our rough calculations, Na_{Zn}, K_{Zn} and Ag_{Zn} are much more stable than Li_{Zn}.

3.4. Vacancy mechanism

Third, we investigate the vacancy-assisted mechanisms of Li, Na, K and Ag diffusion for the −1 charge state. In the vacancy-assisted mechanism, the substitutional dopants (Li_{Zn}, Na_{Zn},

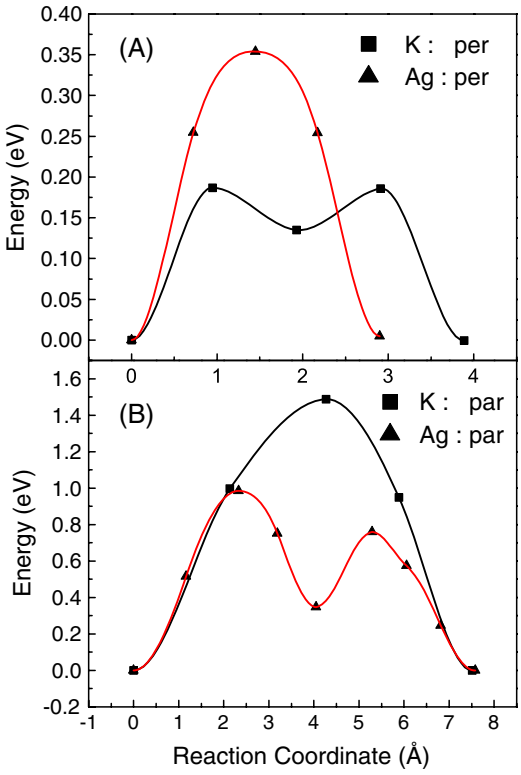

Figure 8. Calculated energy along the migration paths for K and Ag. (A) Perpendicular to the c axis in the same octahedral interstitial cage. (B) Parallel to the c axis.

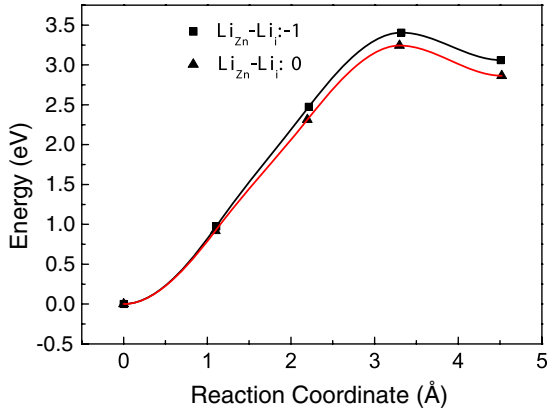

Figure 9. Calculated energy along the migration paths for dissociation processes of Li_{Zn} to Li_i (generating a V_{Zn}) for both the −1 charge state and neutral charge state.

Table 1. All of the calculated energy barriers of Li, Na, K and Ag in wurtzite ZnO.

	Li	Na	K	Ag
Kick-out barrier	2.19	1.60	0.79	1.56
Dissociation barrier	3.41			
Migration barrier ($\perp c$)	0.68	0.74	0.18	0.35
Migration barrier ($\parallel c$)	0.61	1.33	1.49	0.98
Exchange barrier (a)	1.09	1.08	1.21	2.06
Exchange barrier (b)	1.03	1.09	1.30	1.96
Exchange barrier (c)			1.65	1.37
Exchange barrier (d)			1.63	1.43
Exchange barrier (e)	0.74	0.35	0.13	0.42
Exchange barrier (f)	0.74	0.45	0.10(0.44)	0.38(0.76)

K_{Zn} and Ag_{Zn}) diffuse by exchange between the Zn vacancy and the dopant. Due to the well-known correlation factors of vacancy mechanisms [15, 17], the processes for V_{Zn} diffusing, as first-nearest-neighbor, around the dopants is also important, denoted by 'rotation process'. Simply speaking, the jump of the dopant atom is likely highly correlated (i.e. there is a large probability of a back jump), so the correlation factors may be important. Schematic exchange processes and calculated energies along the pathways are plotted in figure 10. We can see that, for Li or Na doping, diffusion of V_{Zn} is almost not changed, whereas for K or Ag doping, diffusion of V_{Zn} can be retarded, where the energy barrier of V_{Zn} under p-type condition is about 1.1 eV [16]. The energy barrier of Li and Na for in-plane exchange (e) is 0.74 eV and 0.35 eV, and for out-of-plane exchange (f) is 0.74 eV and 0.45 eV, respectively. For K and Ag, the in-plane exchange energy barrier is rather small, 0.13 eV and 0.42 eV, respectively. For out-of-plane exchange, the energy barrier of process f is 0.10 eV for K, 0.38 eV for Ag, and the energy barrier of the reverse process of f is 0.44 eV for K and 0.76 eV for Ag. The binding energy is essential for understanding the vacancy mechanisms. The calculated binding energy of out-of-plane Li–V_{Zn}, Na–V_{Zn}, K–V_{Zn} and Ag–V_{Zn} pairs for the +1 charge state is 0.27, 0.29, −0.32 and −0.45 eV, in which the negative value indicates attractive interaction, estimated by the energy difference between the total energy of the 192-atom supercell with a dopant–vacancy pair and a dopant with the furthest zinc vacancy in the 192-atom supercell. All calculated energy barriers are summarized in table 1. Because the energy barrier of the dopant–vacancy exchange (e, f) is much smaller than the energy barrier of the exchange process between vacancy and first-nearest-neighbor Zn of the dopant (a, b, c, d), due to correlation factors, the dominant processes are the latter processes (a, b, c, d) or the dissociation energy barrier of the dopant–vacancy pair, see [17]. The dominant process is actually the process which has the smallest energy barrier of so-called rotation processes and dissociation processes. For K and Ag, as shown in figure 10(D), there are two types of dopant–vacancy pair, which have different binding energies. For computational reasons (the need to use a 192-atom supercell to do CI-NEB calculations), the dissociation processes are excluded from our consideration. On the other hand, because there are two types of dopant–vacancy pair, some processes become nonequivalent and the computation time would increase a lot. We limit ourselves to the dopant–vacancy exchange process and 'rotation process'. Because we have not investigated all relevant processes for the vacancy mechanism, no conclusive results have been reached. It is necessary to pursue further investigations.

In addition, we also investigated the binding energy of a substitutional dopant (Li_{Zn}, Na_{Zn}, Ag_{Zn}, K_{Zn} and Rb_{Zn}) and oxygen vacancy at the −1 charge state, estimated by the energy difference between the total energy of the 192-atom supercell with a dopant–vacancy pair and a dopant with the furthest oxygen vacancy in the 192-atom supercell (LDA). The calculation results are as follows: 1.20 eV, 1.23 eV, 1.74 eV,

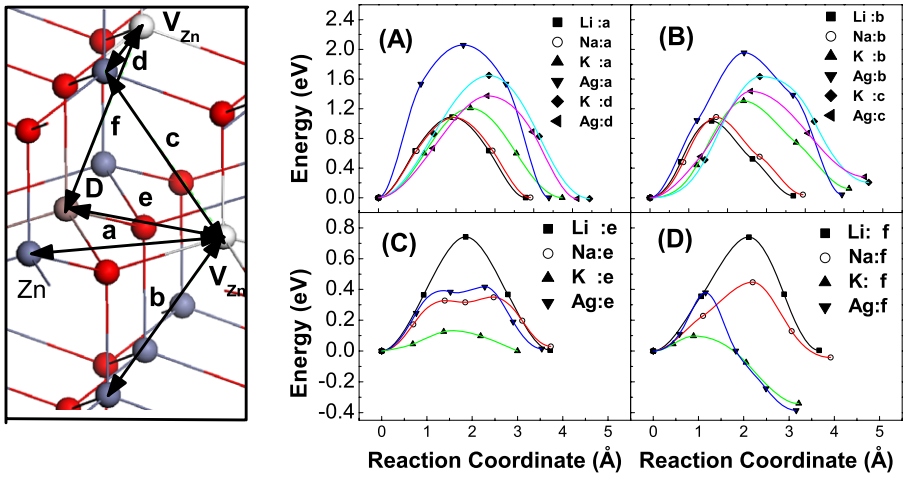

Figure 10. Calculated energy along the migration path. (A) and (B): exchange of Zn–V_{Zn} around the dopant. (C) and (D): exchange of dopant–V_{Zn}. a–f denote the exchange processes shown on the left-hand side.

2.10 eV and 2.59 eV for Li_{Zn}, Na_{Zn}, Ag_{Zn}, K_{Zn} and Rb_{Zn} dopant–vacancy pairs, respectively. We can see that the larger the atomic radius, the larger the binding energy of the dopant–vacancy pair. For all of these dopants, the binding energy is not small, at least 1.20 eV. It indicates that all of them should suffer from the compensation effects of the oxygen vacancy, not just Ag_{Zn}, K_{Zn} and Rb_{Zn}, from an equilibrium point of view.

4. Summary and discussion

In summary, dopant interstitials are found to not easily occupy the substitutional site via kicking the neighboring zinc atom out, at least 1.56 eV energy for Li, Na and Ag, as well as 0.79 eV for K. It indicates that if they are introduced initially in an interstitial site, they are difficult to transform to a substitutional site. These results can explain that, to date, it has not been successful to obtain p-type doping in ZnO by Li, Na, K or Ag doping via ion implantation [20] or diffusion doping, though the growth doping methods are more or less successful. The isolated substitutional dopants are found to be stable. It indicates that, if there are no other point defects present nearby, the substitutional configuration is rather stable. We found there is a large binding energy between the substitutional dopant and the zinc interstitial or oxygen vacancy. Both zinc interstitial and oxygen vacancy, under p-type conditions, play an n-type donor role. The combination between the dopant and zinc interstitial or oxygen vacancy would not directly decrease the concentration of holes, but would decrease the concentration of the isolated zinc interstitial or oxygen vacancy, and make them in a nonequilibrium concentration (less than equilibrium concentration). For all of these dopants, the binding energy with an oxygen vacancy is not small, at least 1.20 eV. It indicates that all of them should suffer from the compensation effects of an oxygen vacancy, not just Ag_{Zn}, K_{Zn} and Rb_{Zn}, from an equilibrium point of view. On the one hand, the oxygen vacancy does not diffuse very fast, with about a 1.4 eV energy barrier [19]. The nonequilibrium concentration of oxygen vacancies may be able to be maintained for a while. On the other hand, a zinc interstitial is a very fast diffuser, with about a 0.5 eV energy barrier [16]. However, the formation energy of a zinc interstitial is very large [14], so the equilibrium concentration is low, and compensation effects should not be large, based on an equilibrium point of view. Nevertheless, a zinc interstitial can kick the dopant to an interstitial site easily and generates a dopant interstitial. Our calculation results indicate that all of the interstitial dopants (Li, Na, K and Ag) are fast diffusers. The generated dopant interstitials cause the concentration to exceed the equilibrium concentration. The excess Li, Na, K or Ag interstitials would diffuse out of the sample. For Na, K and Ag interstitials, the diffusion is highly anisotropic, that is to say, diffusion perpendicular to the *c* axis is easy, whereas diffusion parallel to the *c* axis is not easy (>1 eV). The substitutional dopant can also diffuse via a vacancy mechanism (exchange with a zinc vacancy). We found the exchange barrier between the dopant and zinc vacancy is small. Due to correlation factors [17], the dominant processes are the dissociation processes of dopant–vacancy pairs, or the 'rotated' processes of the zinc vacancy around the dopant. For computational reasons, the dissociation processes are excluded from our considerations here. We have investigated both the exchange processes and the rotation processes. These processes are essential for the vacancy mechanism.

5. Conclusion

In conclusion, we found Li, Na and Ag interstitials are stable with at least a 1.56 eV energy barrier, whereas the K interstitial is relatively thermally unstable with a 0.79 eV energy barrier. It indicates that the Li_{Zn}, Na_{Zn} and Ag_{Zn} may not reach equilibrium concentration at room temperature, if they are introduced initially as interstitials. The isolated dopant substitutional defects (Li_{Zn}, Na_{Zn}, K_{Zn} and Ag_{Zn}) are rather stable, with at least a 3.4 eV energy barrier. All of the dopant interstitials are fast diffusers. It indicates that the concentration of these dopant interstitials is proposed to be in equilibrium at room temperature. The diffusion of the Li interstitial is isotropic, whereas diffusion of Na, K and Ag interstitials is highly anisotropic. Energy barriers of the

fundamental processes of the vacancy-assisted mechanisms are systematically calculated, where the specific values of the corresponding energy barriers and binding energy can be used as the input parameters for relevant diffusion simulations. These results give a good understanding of the diffusion and doping behaviors of group I elements in ZnO.

Acknowledgment

The work is supported by 973 Project (Ministry of Science and Technology of China, grant no. 2006CB605102).

References

[1] Ozgur U, Alivov Y I, Liu C, Teke A, Reshchikov M A, Dogan S, Avrutin V, Cho S J and Morkoc H 2005 *J. Appl. Phys.* **98** 041301
[2] Kasai P H 1963 *Phys. Rev.* **130** 989
[3] Schirmer O F 1968 *J. Phys. Chem. Solids* **29** 1407
[4] Park C H, Zhang S B and Wei S-H 2002 *Phys. Rev.* B **66** 073202
[5] Wardle M G, Goss J P and Briddon P R 2005 *Phys. Rev.* B **71** 155205
[6] Kresse G and Hafner J 1993 *Phys. Rev.* B **47** 558
[7] Kresse G and Furthmuller J 1996 *Phys. Rev.* B **54** 11169
[8] Perdew J P, Burke K and Ernzerhof M 1996 *Phys. Rev. Lett.* **77** 3865
[9] Blöchl P E 1994 *Phys. Rev.* B **50** 17953
[10] Kresse G and Joubert D 1999 *Phys. Rev.* B **59** 1758
[11] Henkelman G, Johannesson G and Jonsson H 2000 *Progress on Theoretical Chemistry and Physics* (Dordrecht: Kluwer Academic) p 269
[12] Henkelman G, Uberuaga B P and Jonsson H 2000 *J. Chem. Phys.* **113** 9901
[13] http://theory.cm.utexas.edu/henkelman
[14] Janotti A and Van de Walle C G 2007 *Phys. Rev.* B **76** 165202
[15] Fahey P M, Griffin P B and Plummer J D 1989 *Rev. Mod. Phys.* **61** 289
[16] Huang G Y, Wang C Y and Wang J T 2009 *Solid State Commun.* **149** 199
[17] Huang G Y, Wang C Y and Wang J T 2009 *J. Appl. Phys.* **105** 073504
[18] Huang G Y, Wang C Y and Wang J T 2009 *Scr. Mater.* **61** 324
[19] Huang G Y, Wang C Y and Wang J T 2009 *J. Phys.: Condens. Matter* **21** 195403
[20] Moe Borseth T, Tuomisto F, Christensen J S, Skorupa W, Monakhov E V, Svensson B G and Yu Kuznetsov A 2006 *Phys. Rev.* B **74** 161202